Sercan Acarer* and Ünver Özkol

Off-Design Analysis of Transonic Bypass Fan Systems Using Streamline Curvature Through-Flow Method

DOI 10.1515/tjj-2016-0083
Received December 28, 2016; accepted January 19, 2017

Abstract: The two-dimensional streamline curvature through-flow modeling of turbomachinery is still a key element for turbomachinery preliminary analysis. Basically, axisymmetric swirling flow field is solved numerically. The effects of blades are imposed as sources of swirl, work input/output and entropy generation. Although the topic is studied vastly in the literature for compressors and turbines, combined modeling of the transonic fan and the downstream splitter of turbofan engine configuration, to the authors' best knowledge, is limited. In a prior study, the authors presented a new method for bypass fan modeling for inverse design calculations. Moreover, new set of practical empirical correlations are calibrated and validated. This paper is an extension of this study to rapid off-design analysis of transonic by-pass fan systems. The methodology is validated by two test cases: NASA 2-stage fan and GE-NASA bypass fan case. The proposed methodology is a simple extension for streamline curvature method and can be applied to existing compressor methodologies with minimum numerical effort.

Keywords: bypass fan, through-flow, streamline curvature, off-design, performance map

PACS® (2010). Computational techniques/fluid dynamics, 47.11.-j

Introduction

Turbomachinery flows are among the most complicated flows, which dictate the use of low order models at the beginning of design and progressively increasing fidelity through the end of design [1]. Up to 80 % or more of the design parameters may be fixed during mono and two dimensional modeling phases [2]. The two-dimensional streamline curvature through-flow modeling on the turbomachinery meridional (axial-radial) plane, derived from the general S_1/S_2 theory of Wu [3], is still among the key elements in preliminary design [2], off-design analysis and post-processing of test data [1]. In a through-flow solution, basically, the effects of blades are considered in a swirling axisymmetric flow field through empirical correlations. By this way, the global aspects of a turbomachinery flows are considered.

The most common through-flow solution methods for the axisymmetric swirling flow field are the streamline curvature method (SLC) [4–7], the matrix method [8], the finite element method [9, 10], the time-marching Euler method [11–14] and the Reynolds averaged Navier-stokes method [15]. Although the Navier-Stokes solution is the most advanced one, through-flow solution is a meridional plane approximation and the effects of blades are estimated by the help of empirical correlations, not only by the solver itself. Therefore, it is the empirical models which determine accuracy rather than the utilized numerical method. As a result, SLC is the most commonly used method due to its speed and robustness [16].

Due to this aforementioned importance of the empirical models, researchers developed various correlations over the years. Although most of those are confidential, there are some publicly available ones as well, such as those published by Lieblein et al. [17, 18], Miller et al. [19] and Koch&Smith [20]. Improvements to those baseline correlations are mainy made in two areas: Secondary flow treatment and shock losses. Adkins & Smith [21], Gallimore [22], Wisler et al. [23], Dunham [24] and Monig et al. [25] fall into the first category while the studies of Wennerstrom [26] and Boyer [27] fall into the former category. More recently, the authors, in a prior study [28], compiled correlations from the open literature and calibrated them against three test cases. The principal improvement is in the area of shock loss predictions, which is accomplished by extending applicability of the circular-arc supersonic expansion

***Corresponding author: Sercan Acarer,** Department of Mechanical Engineering, İzmir Katip Çelebi University, 35620 Çiğli/İzmir, Turkey, E-mail: sercanacarer@gmail.com
Ünver Özkol, Department of Mechanical Engineering, İzmir Institute of Technology, 35430 Urla/İzmir, Turkey, E-mail: unverozkol@iyte.edu.tr

angle expression to non-circular camberlines. A good agreement with test data is observed.

Despite the cited through-flow literature there is very little discussion related to through-flow modeling of bypass fans. Even less studies deal with SLC modeling of bypass fans. Novak [5] considered solver aspects, without empirical models, while Shan [29] developed a model applicable only to low-bypass turbofan systems. More recently, the authors of this manuscript, Acarer and Ozkol [28], developed an extensive model for design point operation of bypass fan systems. This study is an extension of this prior study to off-design performance prediction applications.

Streamline curvature method for bypass fans

This section aims to summarize the utilized baseline streamline curvature method (SLC) [28]. SLC is based on the inviscid Euler equations, which are cast in streamline coordinates. In the final equation, the gradient of streamline (meridional) velocity along quasi-orthogonals (QO) is considered (Figure 1) [6]:

$$V_m \frac{\partial V_m}{\partial q} = \frac{\partial H}{\partial q} - T\frac{\partial s}{\partial q} - \frac{V_\theta}{r}\frac{\partial (rV_\theta)}{\partial q} - F_q + V_m \sin\varepsilon \frac{\partial V_m}{\partial m} - K_m V_m{}^2 \cos\varepsilon \quad (1)$$

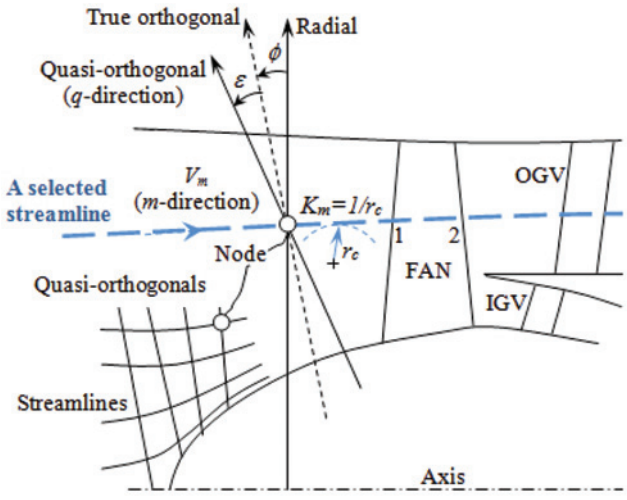

Figure 1: Computational framework [28].

The computational domain is established by number of nodes, which are intersections of streamlines with the predefined QOs. Streamline shapes (nodal positions, local streamline curvature, K_m and slope, ϕ) are required in eq. (1) to obtain a solution. As the streamlines are unknown at the beginning of the solution, they are initially estimated. During a solution, nodes float on the QOs to modify shape of streamlines based on streamtube continuity. Once adjustments are within specified tolerance, the solution is terminated. The equation is accompanied by continuity equation and energy and empirical models for blades, which are considered within total enthalpy (H), swirl (V_θ), entropy (s) and blade force (F_q) terms. Different than the prior study [28], direct (off-design analysis) solution mode is considered in the scope of current study, where blade angles are specified and the solution is sought for the resulting flow field. Readers are referred to Cumpsty [1] and Denton [6] for details of SLC methodology.

The split-flow methodology described in the original paper [28] is applied in this paper. In this methodology; fan (domain 1), bypass (domain 2) and core (domain 3) sub-domains are sequentially solved in a coupled manner. During each subdomain solution, the complete network of streamlines is used instead of only portions of streamlines which are within the considered domain. Moreover, after each fan domain solution, exit flow field is transmitted to bypass and core domains as inlet conditions. With these two steps, complete coupling is accomplished. The scheme and solution algorithms are presented in Figures 2 and 3, respectively.

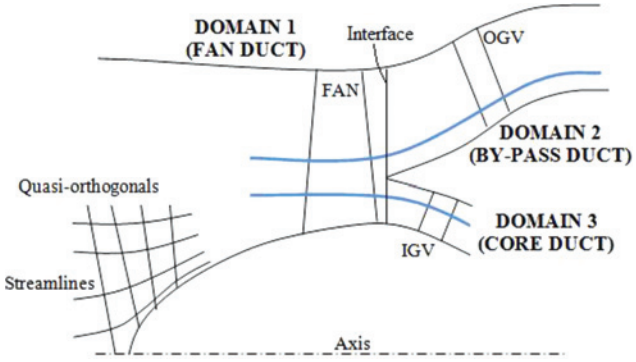

Figure 2: The split-flow scheme [28].

Utilized empirical models

Complete list of the utilized models are listed in Table 1 and the most important aspects of those models are re-described in the following text [28]. The reference minimum loss incidence (i^*) and the corresponding deviation (δ^*) are obtained from the well-known Lieblein models [18, 30]. Once the reference minimum loss incidence is obtained, reference stall and choke angular ranges are

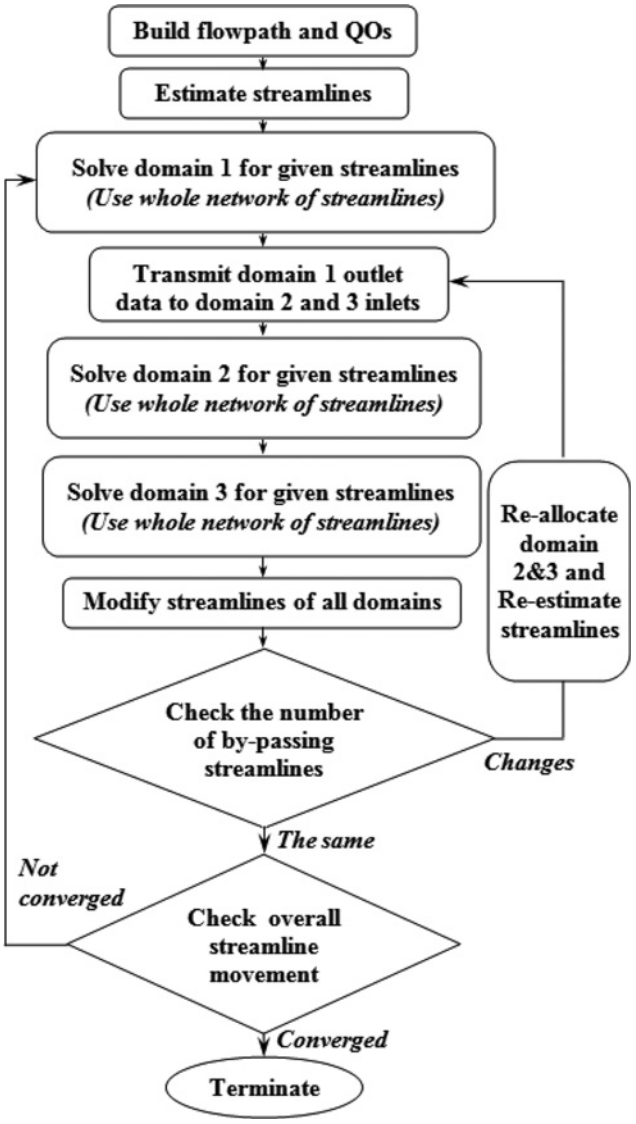

Figure 3: The solution algorithm [28].

estimated to establish compressibility corrections. The range from design incidence to choke incidence (i_c), denoted as R_c, can be estimated from [31]:

$$i_c - i^* = -R_c = -\left(10 - \theta\frac{(K_1 - 40)}{450}\right)\left(0.5 + 5\frac{th}{c}\right) \quad (2)$$

Similarly, reference range from design incidence to stall incidence (i_s), denoted as R_s, can be estimated by:

$$i_s - i^* = R_s = 1.5\left(10 + \theta\frac{(55 - K_1)}{150}\right)\left(0.5 + 5\frac{th}{c}\right) \quad (3)$$

These ranges get considerably narrower as the inlet relative Mach number increases. Aungier [32] suggests below corrections for compressibility effects:

Table 1: Summary of the utilized empirical models [28].

Reference minimum-loss incidence	Lieblein [18] or NASA SP-36 [30]
Ref. stall-choke incidence range	Kleppler [31]
Mach corrected stall-choke range	Aungier [32]
Mach corrected min. loss incidence	Aungier [32]
Reference deviation	Lieblein [18] or NASA SP-36 [30]
Deviation correction	Boyer [27]
Equivalent diffusion factor	Koch& Smith [20]
Friction (profile + secondary) loss coefficient	Aungier [32] (based on NASA SP-36 [30])
Transonic shock loss coefficient	Aungier [32]
Supersonic shock loss coefficient	Miller et.al [19] and Wennerstrom [26]
End-wall blockage	Pachidis [33]
Off-design loss	Çetin et.al [34]
Off-design deviation	Creveling [35]

$$i_{c\ (compressible)} = i^* - R_c / \left[1 + 0.5(M_1')^3\right] \quad (4)$$

$$i_{s\ (compressible)} = i^* + R_s / \left[1 + 0.5(K_{sh}M_1')^3\right] \quad (5)$$

Finally, Mach-corrected minimum loss incidence is obtained by [32]:

$$i_m = i_c + (i_s - i_c)R_c/(R_c + R_s) \quad (6)$$

For the deviation (δ^*), a correction is also applied for meridional acceleration or deceleration, which has a significant impact [27]:

$$\delta_{V_m} = 10(1 - V_{m2}/V_{m1}) \quad (7)$$

This modification is limited to ±5 degrees. The total pressure loss coefficient, defined as the ratio of relative total pressure loss to inlet relative dynamic pressure, is composed of friction (profile + secondary) and shock loss coefficients. The friction loss coefficient is based on NASA SP-36 loss correlations [30], defined by:

$$\varpi^* = \frac{2\sigma C_1\left[C_2 + 3.1(D_{eq} - 1)^2 + 0.4(D_{eq} - 1)^8\right]}{\cos(\beta_2)}\left(\frac{W_2}{W_1}\right)^2 \quad (8)$$

Where C_1 and C_2 are calibration coefficients and σ is solidity. C_1 is selected as 0.0073 [32], while C_2 is calculated by [32]:

$$C_2 = 1 + (t_{average}/h)\cos\beta_2 \quad (9)$$

The friction loss coefficient, defined by eq. (8), is corrected for Mach number effects as:

$$\varpi_{friction} = \varpi^*\left[1 + (i_m - i^*)^2/R_s{}^2\right] \quad (10)$$

Shock losses are considered both for transonic-inlet and supersonic-inlet sections. For transonic-inlet sections, below relation is used [32]:

$$\varpi_{shock(transonic)} = K_{sh}[(M_1'/M_{critical} - 1)W_{sonic}/W_1]^2 \quad (11)$$

For supersonic-inlet sections, Miller-Lewis-Hartmann (MLH) model [19] is used as a baseline to calculate shock losses ($\varpi_{PT\text{-}shock(supersonic)}$). In this model, the shock is assumed to be normal at the line connecting leading edge and suction side, where the line is normal to the suction side (Figure 4). This is a condition close to peak efficiency condition and all the neglected effects (the oblique shocks, leading edge bluntness, precise location of the shock, etc.) are lumped into this normal shock through a proper model calibration process.

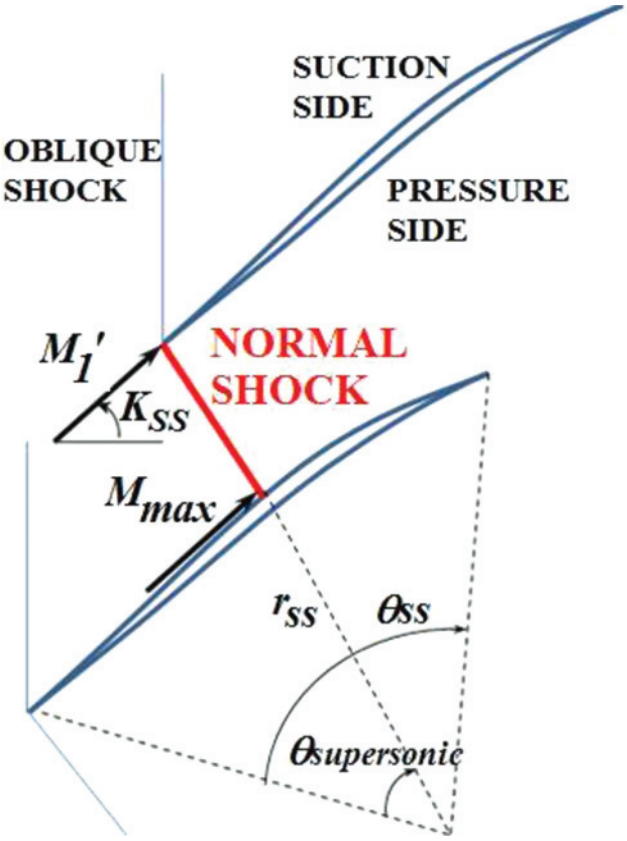

Figure 4: Visualization and nomenclature of the shock loss model.

The model assumes that the normal shock loss can be estimated by a representative Mach number, which is average of the inlet relative Mach number and accelerated suction side flow (Figure 4). Different than the original MLH model [19], where the representative Mach number is the arithmetic average of the two Mach numbers, Aungier [32] suggests geometric averaging should be done for better accuracy, as incorporated in this study. In addition, the present study utilizes the model of Wennerstrom [26] to take into account spanwise obliqueness of the shock surface. This is done by multiplying both inlet relative Mach number and maximum suction surface Mach number by sine of the leading edge and shock impingement (point of M_{max}) obliqueness angles ($\alpha_{obliqueness}$), respectively. In conclusion, the representative Mach number is:

$$M_{SHOCK} = \sqrt{M_1' M_{max} \left|\sin(\alpha_{obliqueness})\right|_{leadingedge} \left|\sin(\alpha_{obliqueness})\right|_{impingementpoint}} \quad (12)$$

To estimate M_{max}, the suction side acceleration is estimated by a Prandtl-Mayer expansion angle ($\theta_{supersonic}$) (Figure 4) (see any elementary text book on compressible flows). But, such an expansion has to be estimated on a circular camberline (e. g. DCA blades) in the correlation. The estimated expansion is modified for real supersonic camberlines (MCA or wedge blades) as a function of inlet relative Mach number, as described in the last paragraph of this section. The equations leading to $\theta_{supersonic}$ for a circular arc camberline are [32]:

$$\tan(\theta_{SS}/4) = \tan(\theta/4) + \frac{th}{c} \quad (13)$$

$$r_{SS} = \frac{c}{2\sin(\theta_{SS})} \quad (14)$$

$$K_{SS} = 90 - \frac{\theta_{SS}}{2} - K_1 + \frac{\theta}{2} \quad (15)$$

$$\theta_{supersonic} = \arctan\left(\frac{t\cos(K_{SS})}{t\sin(K_{SS}) + r_{SS}}\right) \quad (16)$$

The obliqueness angle at the leading edge is calculated from:

$$\alpha_{obliqueness\,(Leadingedge)} = \arccos(\cos\beta_1 \cos(lean)\sin(\varepsilon) - \sin\beta_1 \sin(lean)) \quad (17)$$

The calculation at the impingement point is difficult to obtain. A rather simple approach is used here as this only has a minor effect. If blade span is defined from 0 (hub) to 1 (tip), it is assumed that the impingement point obliqueness is equal to the leading edge obliqueness for span<0.5. As for the span ≥ 0.5, then the impingement point obliqueness is assumed to be two times the leading edge obliqueness. This is correlated from typical fan or compressors that the authors experienced.

Once the maximum suction side Mach number is calculated using $\theta_{supersonic}$ and the representative shock

Mach number is estimated, the generic 1D normal shock relation is used to estimate relative total pressure loss due to the shock. Finally, it must be converted to the total pressure loss coefficient form [32].

The off-design correlations derived by Cetin et. al [34]. and Creveling [35] are used to treat off-design loss and deviation. For MCA profiles, below relations are given:

$$c_m = 0.02845M_1' - 0.01741\ (incidence < i_m) \tag{18}$$

$$c_m = 0.00363M_1' - 0.00065\ (incidence > i_m) \tag{19}$$

For DCA profiles, below relations are used:

$$c_m = 0.05336M_1' - 0.02937\ (incidence < i_m) \tag{20}$$

$$c_m = 0.00500M_1' - 0.00075\ (incidence > i_m) \tag{21}$$

Finally, the off-design loss coefficient is given by the below relation:

$$\varpi_{off-design} = \varpi_{friction} + c_m(incidence - i_m)^2 + \varpi_{shock} \tag{22}$$

For off-design deviation angle, Cetin et. al [34]. recommends, after testing the performance of many alternative off-design deviation angle correlations, the correlation derived by Creveling [35]:

$$eps = K_1 - K_2 - \delta_m + i_m \tag{23}$$

$$PP_1 = (incidence - i_m)/eps \tag{24}$$

If PP_1 is positive, then the coefficients are: $d_1 = -0.2928$, $d_2 = 0.5588$ and $d_3 = -0.000809$. If PP_1 is negative, then $d_1 = -0.3452$, $d_2 = 0.4800$ and $d_3 = 0.0001191$. Those coefficients are used in the below equation:

$$PP_2 = d_1 PP_1^{\,2} + d_2 PP_1 + d_3 \tag{25}$$

Finally, the off-design deviation is given by:

$$\delta_{off-design} = \delta_m + eps\, PP_2 \tag{26}$$

Even if these utilized correlations, which are summarized in Table 1 with references to original sources, were developed from extensive compressor cascade tests and therefore well-established, without any change in the overall structure, a calibration of some constants is deemed necessary to apply them to bigger-scale transonic fans. Such calibration was made for peak efficiency operating points of NASA 2-stage fan and a custom designed transonic fan stage simultaneously, and then the performance of the final calibration for these two transonic fans was successfully tested at peak efficiency operating point of GE-NASA transonic bypass fan in the prior work [28]. First of all, the pitch of a section is calculated at the leading edge radial position (relative to machine axis) while solidity is calculated at mid-chord radial position. The second enhancement is that, if overturning occurs (roots of fans), exit metal angle is taken as zero instead of negative value. This is due to the assumption that incidence is mostly affected by leading edge region rather than the exit overturning region. Moreover, the correlations are valid for cases without overturning. In this regard, authors experienced better match in NASA 2-stage fan test case. The third enhancement is that, the exponent '2' in eq. (11) is made '1.6' to better match test cases. The fourth enhancement is that suction surface Prandtl-Mayer expansion is reduced relative to a circular-arc expansion. The circular-arc expansion (for given inlet and outlet angles) is multiplied by 0.95 for inlet relative Mach number smaller than 1.25, multiplied by 0.45 for inlet relative Mach number bigger than 1.40 and a linear distribution is assumed in between these two Mach numbers. This is the most important modification towards higher accuracy [28]. Its justification comes from the fact that Prandtl-Meyer expansion for circular camberlines ($\theta_{supersonic}$ estimated in eq. (16)) are too high (and yields excessively over-predicted shock losses) for real transonic or supersonic blades, which have rather flat inlets to reduce this expansion. The fifth (and the last) enhancement is related to deviation angle, which is reduced by 1° relative to predicted values. Moreover, for rotors, an additional 2° tip deviation is added, which diminishes at 90 % span. With those modifications, the authors experienced better match with test cases [28].

Validation with NASA 2-stage fan

This section presents validation of the code with NASA 2-stage fan with wide-chord 1st stage rotor, reported in reference [36]. The main parameters are given in Table 2. The meridional view of the fan and QOs are presented in Figure 5. The 1st stage rotor and tip sections of the 2nd stage rotor are made of multiple-circular-arc (MCA) profiles, where maximum thickness locations are shifted

Table 2: Overall properties of NASA 2-stage fan at peak efficiency point.

	Overall	Stage 1	Stage 2
Total pressure ratio	2.471	1.655	1.494
Adiabatic efficiency	0.846	0.87	0.842
Mass flow [kg/s]		34.03	
Revolutions per minute		16083.8	

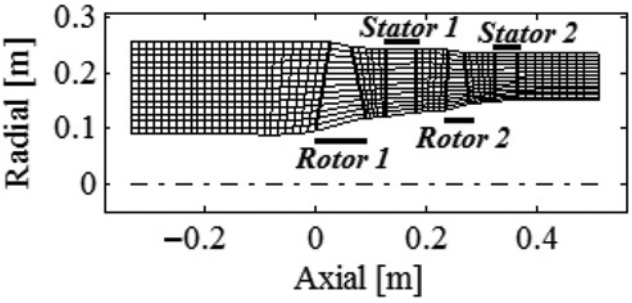

Figure 5: Meridional view and SLC grid.

rearwards to reduce supersonic expansion. Lower sections of 2nd stage rotor and all stators are made of double-circular-arc (DCA) profiles.

Boundary conditions given are mass flow rate and spanwise distributions of total pressure and temperature at the inlet; and blade angle spanwise distributions at the inlet and exit of each blade row. Cubic splines are used for interpolation along the span.

Performance maps are presented in Figures 6 and 7, where decent agreements with test data [36] are observed for such a rapid prediction tool. At 100 % corrected speed, very good agreement is observed, however, for lower speeds, agreement is worse. One reason of this may be the fact that off-design correlations of Çetin et al. [34] are valid for high-speed applications. At lower speeds, discrepancies may increase. Moreover, NASA 2-stage fan, due to being a research fan that pushes conventional (safe) loading limits, has highly loaded stators with around 60 degree total metal turning and 15 degree overturning (the part of the total turning that

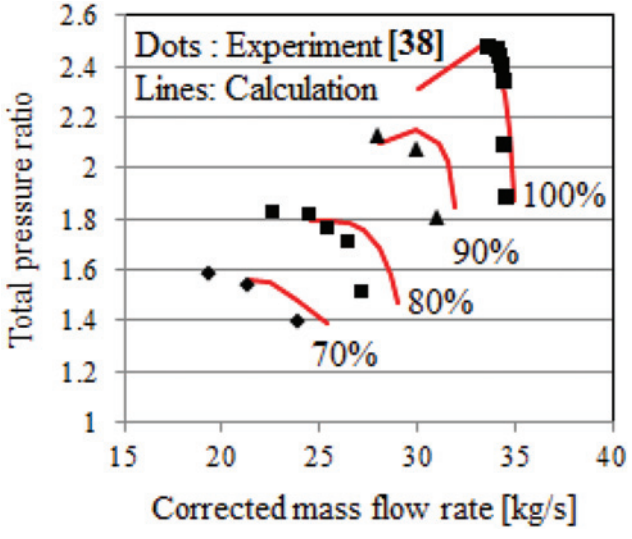

Figure 6: Total pressure ratio.

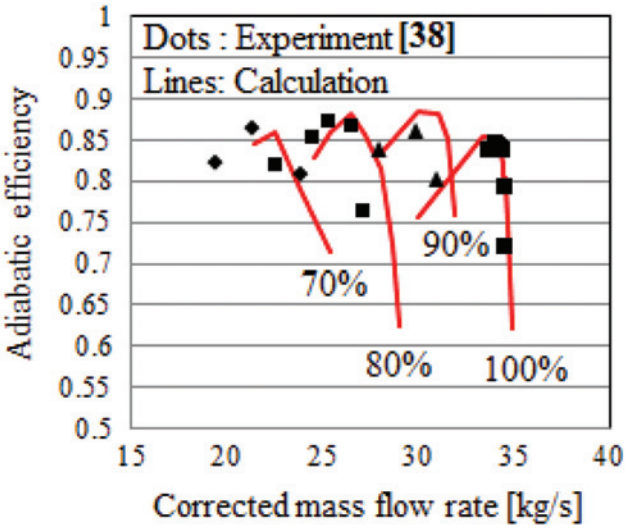

Figure 7: Adiabatic efficiency.

is beyond making the flow axial) [36]. Therefore, this may create stronger-than-conventional 3D secondary flow and blockage, which are challenging to obtain good estimation for the simple correlations used in the presented through-flow solver. Therefore, it is expected that the code may perform even better for more conventionally designed fans. It can be concluded that, based on this test case, higher rotational speed regions are better captured by the methodology.

Validation with GE-NASA bypass fan

This section presents validation of the code with GE-NASA bypass fan, whose design procedure is reported in reference [37] and test data is documented in reference [38]. The global experimental performance is given in Table 3 for short bell-mouth inlet configuration. Uniform inlet tests with long bell-mouth inlet, where the majority of data points are collected, are selected for benchmarking, however, short bell-mouth

Table 3: Overall properties of GE bypass fan at peak efficiency point with short bellmouth inlet [37, 38].

	Fan rotor	Bypass stage	Core stage
Total pressure ratio	1.770	1.757	1.642
Adiabatic efficiency	0.857	0.829	0.826
Mass flow [kg/s]		114.55	
Bypass ratio		5.88	
Revolutions per minute		10622.3	

results are also presented. All the comparisons are performed at the nominal bypass ratio of 6.

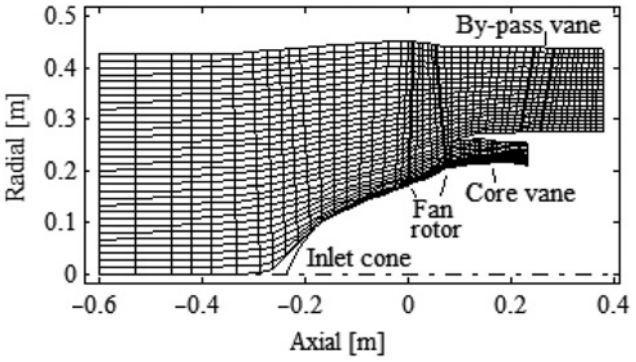

Figure 8: Meridional view and SLC grid.

The meridional view of the fan and QO's are presented in Figure 8. The rotor is made of custom tailored blades. Towards the tip section, where supersonic inlet relative Mach numbers are encountered, maximum turning point moves rearward to reduce shock losses. This effect is already modeled by the shock-loss enhancement described in the last paragraph of Section "Utilized empirical models" for design point operation (and its success is already demonstrated in the prior paper for design point operation [28]). For off-design operation, which is the topic of this paper, the additional off-design corrections given in eqs (18)–(21) are implemented to the methodology for DCA and MCA blades. The off-design corrections for double-circular-arc (DCA) sections given by eqs (20) and (21) are not suitable to model those supersonic profiles (because DCA blades are mid-loaded blades). Although the blades are not standard profiles, flat (wedge-like-shaped) suction side inlet and the placement of maximum turning through the rear of the sections is the characteristic of multiple-circular-arc blades (MCA). Actually the purpose of MCA profiles is to model such aft-loaded transonic or supersonic blades [34]. Therefore MCA blade off-design corrections given by eqs (18) and (19) are used for the rotor. The bypass outlet guide vanes (OGV) are made of DCA profiles and the core inlet guide vanes (IGV) are made of NACA 65 profiles.

In Figure 9, fan pressure ratio map is presented. Agreement is generally decent. At 100 % speed-line, choke mass flow cannot be captured but there are uncertainties related to modelling simplicity. GE also predicted a higher design mass flow rate of 117.9, whereas tests revealed that only 113.84 kg/s mass flow rate passes with long bell-mouth inlet and 114.55 kg/s mass flow rate

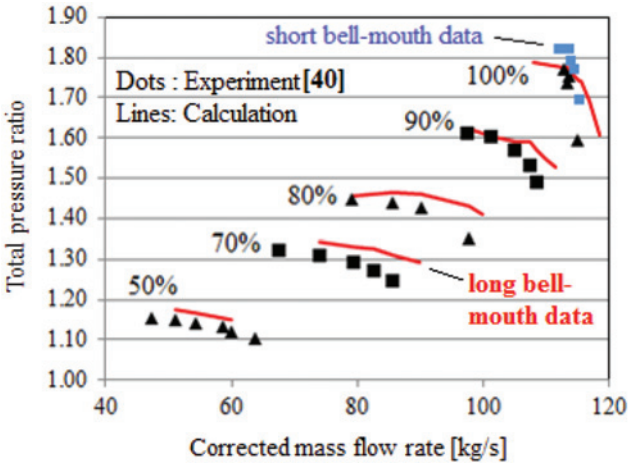

Figure 9: Fan rotor pressure ratio.

passes with short bell-mouth inlet. Differences are mainly attributed to instrumentation and mispredicted deformation of the rotor with rotation. In light of these considerations, it is assessed that agreement is decent at high rotational speeds where inlet relative Mach numbers are transonic or supersonic and therefore off-design correlations of Cetin et al. [34] are valid. The corresponding efficiency graph is presented in Figure 10. Efficiency levels (or at least trends) are generally well predicted for this case.

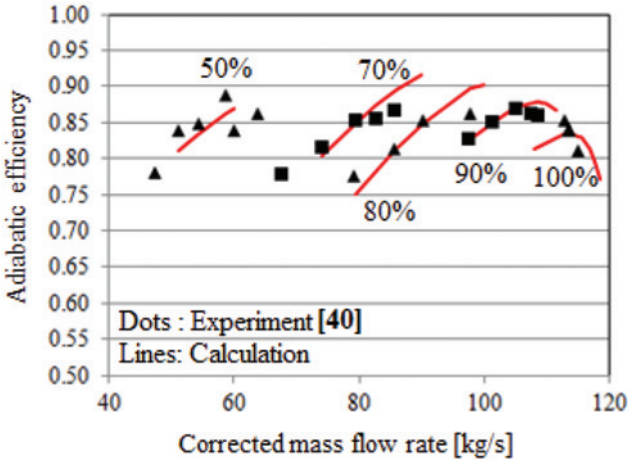

Figure 10: Fan rotor efficiency.

In Figure 11, bypass pressure ratio map is presented. Contrary to the fan-only case, choke mass flow rate at 100 % speed-line is better predicted. The errors in fan calculations seem to be compensated by the errors in bypass OGV calculations. Comparisons at other rotational speeds possess accuracy levels that are similar with fan-

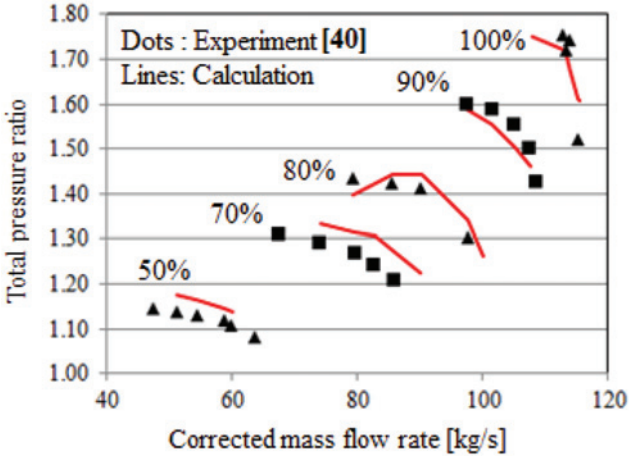

Figure 11: Bypass pressure ratio.

only predictions. The corresponding efficiency levels are presented in Figure 12. The absolute values of the efficiency levels are generally around 5–10 % mispredicted for the bypass stage at high rotational speeds compared to test data [38]. All through-flow methods are steady two-dimensional methods and losses arising from complex coupled unsteady three-dimensional flow structures (hub secondary flows, tip leakage, shock-boundary layer interaction, shock-tip leakage interaction, unsteady rotor-stator interactions, mixing between rotor-stator, interactions of those losses with hub and shroud walls) [1] can only be estimated roughly by simple empirical correlations derived from two-dimensional cascade experiments. These losses may not always be perfectly captured by the simple correlations and this translates into errors in efficiency predictions. This is also stated by Casey et al. [39], who therefore suggested using as many additional monitors as possible, other than efficiency (like diffusion factor, maximum relative Mach number, etc. that have influence on efficiency), for efficiency-potential comparison of rival designs in through-flow based optimization practices. Also, the aforementioned uncertainty arising from untwist (metal deformation under rotation) of the high-aspect-ratio (height/chord) rotor may contribute significantly to this misprediction through accumulation of errors through successive blade rows. Nonetheless, even if the absolute efficiency values are mispredicted, overall trends seem to be captured.

In Figures 13 and 14, core pressure ratio and efficiency maps are presented. The agreement, especially at 100 % speed-line, is worse for this case. It is evident that (at least the utilized) through-flow approximation is not successful in resolving complex three-dimensional flow field in fan roots [40]. This region can best be resolved by a three-dimensional Navier-Stokes solution.

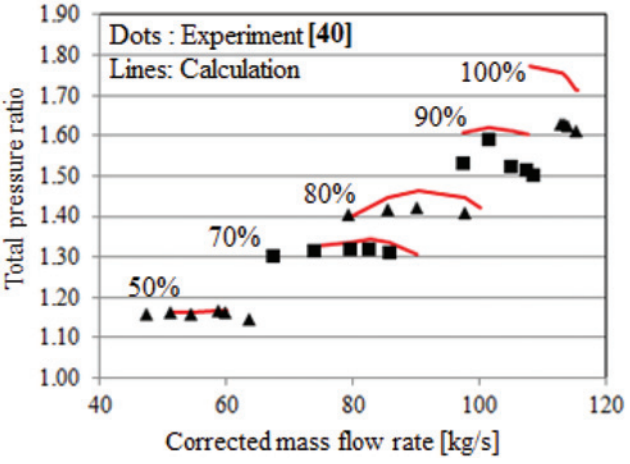

Figure 13: Core pressure ratio.

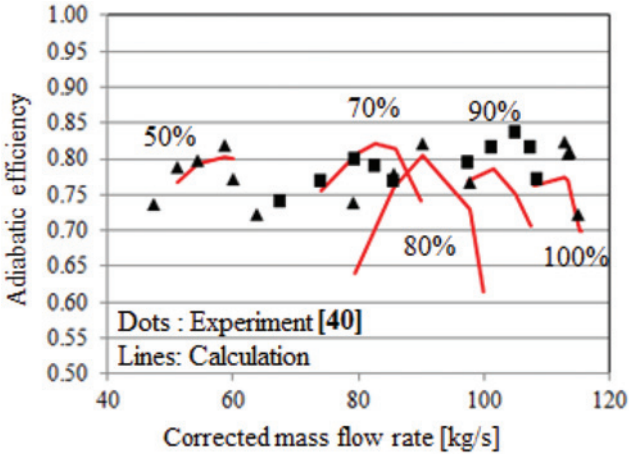

Figure 12: Bypass efficiency.

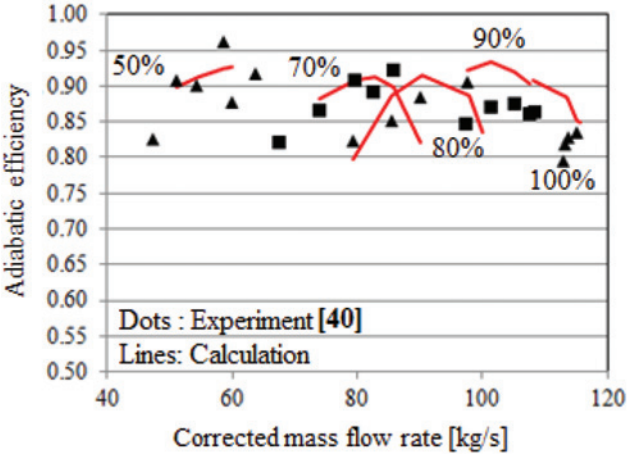

Figure 14: Core efficiency.

Conclusions

A through-flow program has been developed for rapid off-design analysis of transonic fan systems with emphasis placed on bypass fans, a topic which is not considered in detail in the open literature. Empirical models for minimum-loss incidence, deviation, total pressure loss and end-wall blockage were gathered from the open literature and calibrated with experimental and numerical data of transonic fans in a prior study for design point operation. In this study, performance of those models is tested in off-design operations of NASA 2-stage fan and GE-NASA bypass fan. Both fans are transonic with inlet tip relative Mach numbers of 1.4 and 1.6, respectively. For such challenging cases, it has been shown that decent agreement is observed for a rapid prediction tool.

The developed methodology is a simple extension of streamline curvature through-flow method and can be implemented to existing codes for performance map prediction and early component matching studies.

Acknowledgements: Authors would like to thank Tusaş Engine Industries (TEI) for their support for this work.

Funding: The author(s) received no financial support for the research, authorship, and/or publication of this article.

Nomenclature

θ_{SS}	Suction surface camber angle [°]
ε	Angle between true and quasi orthogonals [°]
θ	Camber angle [°]
δ	Deviation angle [°]
ϖ	Mach corrected relative total pressure loss coefficient
σ	Solidity
ϕ	Streamline slope with respect to machine axis [°]
ϖ^*	The reference (low speed) design pressure loss coefficient
δ_m	Deviation angle corresponding to i_m [°]
$\alpha_{obliqueness}$	Local obliqueness angle of the shock surface [°]
$\theta_{supersonic}$	Suction surface camber angle between inlet and the shock location [°]
c	Chord [m]
C_1, C_2	Coefficients in loss correlation
c_m	Coefficient in off-design loss
d_1, d_2, d_3	Coefficients in off-design deviation
D_{eq}	Equivalent diffusion factor
eps	Coefficient in off-design deviation
F_q	Blade force along quasi-orthogonal [N]
H	Total enthalpy [J/kg]
i^*	The reference (low speed) design incidence [°]
i_c	The reference (low speed) choke incidence [°]
i_m	Mach corrected design incidence [°]
i_s	The reference (low speed) stall incidence [°]
K	Metal angle [°]
K_B	Blockage factor (available area /total area)
K_m	Streamline curvature ($=1/r_c$)
K_{SS}	Suction surface inlet metal angle [°]
M	Mach number
PP_1, PP_2	Coefficients in off-design deviation
q	Quasi-orthogonal direction
r	Radial position [m]
r_c	Streamline radius of curvature [m]
R_c	The range from design to choke incidences [°]
R_s	The range from design to stall incidences [°]
r_{SS}	Suction surface radius of curvature [1/m]
s	Entropy [J/kgK]
t	Pitch between two blades [m]
T	Static temperature [K]
th	Profile maximum thickness [m]
V	Absolute velocity [m/s]
W	Relative velocity [m/s]

Subscripts

m	Meridional (streamline) direction
θ	Tangential direction
$1, 2$	Leading and trailing edge of a section, respectively

Superscripts

’	Relative

Abbreviations

CFD	Computational fluid dynamics
DCA	Multiple-circular-arc
IGV	Inlet guide vane
MCA	Double-circular-arc
OGV	Outlet guide vane
QO	Quasi-orthogonal
SLC	Streamline curvature method

References

1. Cumpsty NA. Compressor aerodynamics, 5th ed. Florida, USA: Krieger Publishing Company, 2004.
2. Shahpar S. Optimisation strategies used in turbomachinery design from an industrial perspective. *VKI Lecture Series*, 2010.
3. Wu CH. A general theory of three-dimensional flow in subsonic and supersonic turbomachines of axial, radial and mixed-flow types. NACA TN-2604, 1952.
4. Smith LH. The radial-equilibrium equations of turbomachinery. J Eng Power 1966;88:1–12.
5. Novak RA. Streamline curvature computing procedures for fluid flow problems. Trans ASME J Eng Power 1967;89:478–90.
6. Denton J. Throughflow calculations for transonic axial flow turbines. J Eng Power 1978;100:212–8.
7. Tiwari P, Stein A, Lin Y. Dual-solution and choked flow treatment in a streamline curvature throughflow solver.

Proceedings of ASME Turbo Expo 2011, Vancouver, Canada, 2011.
8. Marsh H. A digital computer program for the through-flow fluid mechanics in an arbitrary turbomachine using a matrix method. British Aeronautical Research Council Reports and Memoranda R. & M. No. 3509, 1968.
9. Hirsch C, Warzee G. An integrated quasi-3D finite element calculation program for turbomachinery flows. J Eng Power 1979;101:141–8.
10. Petrovic M, Wiedermann A, Banjac M. Development and validation of a new universal through flow method for axial compressors. Proceedings of ASME Turbo Expo 2009, Orlando, USA, 2009.
11. Spurr A. The prediction of 3D transonic flow in turbomachinery using a combined throughflow and blade-to-blade time marching method. Int J Heat Fluid Flow 1980;2:189–99.
12. Sturmayr A. Evolution of a 3D structured Navier-Stokes solver towards advanced turbomachinery applications. PhD Thesis, University of Vrije, 2004.
13. Taddei SR, Larocca F, Bertini F. Euler inverse axisymmetric solution for design of axial flow multistage turbomachinery. Proceedings of ASME Turbo Expo 2010, Glasgow, UK, 2010.
14. Gu F, Anderson M. CFD-based throughflow solver in a turbomachinery design system. Proceedings of ASME Turbo Expo 2007, Montreal, Canada, 2007.
15. Simon J. Contribution to throughflow modeling for axial-flow turbomachines. PhD Thesis, University of Liege, 2007.
16. Casey M, Robinson C. A new streamline curvature throughflow method for radial turbomachinery. Proceedings of ASME Turbo Expo 2008, Berlin, Germany, 2008.
17. Lieblein S, Roudebush WH. Theoretical loss relations for low-speed two dimensional cascade flow. NACA TN 3662, 1956.
18. Lieblein S. Incidence and deviation-angle correlations for compressor cascades. Trans ASME J Basic Eng 1960;82:575–84.
19. Miller G, Lewis G, Jr., Hartmann M. Shock losses in transonic compressor blade rows. J Eng Power 1961;83:235–42.
20. Koch C, Smith L. Loss sources and magnitudes in axial-flow compressors. J Eng Power 1976;98:411–24.
21. Adkins G, Smith L. Spanwise mixing in axial-flow turbomachines. J Eng Power 1982;104:97–110.
22. Gallimore S. Spanwise mixing in multistage axial flow compressors: part II – throughflow calculations including mixing. J Turbomach 1986;108:10–16.
23. Wisler D, Bauer R, Okiishi T. Secondary flow, turbulent diffusion, and mixing in axial-flow compressors. J Turbomach 1987;109:455–69.
24. Dunham J. Modelling of spanwise mixing in compressor through-flow computations. Proc Inst Mech Eng 1997;211: 243–51.
25. Mönig R, Mildner F, Röper R. Viscous-flow two-dimensional analysis including secondary flow effects. J Turbomach 2001;123:558–67.
26. Wennerstrom AJ. Design of highly loaded axial-flow fans or compressors. Vermont, USA: Concepts Eti, 2001.
27. Boyer KM. An improved streamline curvature approach for off-design analysis of transonic compression systems. PhD Thesis, Virginia Polytechhnic Institute and State University, 2001.
28. Acarer S, Ozkol U. An extension of the streamline curvature through-flow design method for bypass fans of turbofan engines. Proc IMechE Part G J Aerosp Eng 2017. DOI:10.1177/0954410016636159. (In Press).
29. Shan P. A mass addition approach to the bypass turbomachine through flow inverse design problem. J Mech Sci Technol 2008;22:1921–5.
30. Bullock R, Johnsen I. Aerodynamic design of axial flow compressors. NASA SP36, 1965.
31. Kleppler J. Technique to predict stage-by-stage, pre-stall compressor performance characteristics using a streamline curvature code with loss and deviation correlations. MSc Thesis, University of Tennessee, 1998.
32. Aungier RH. Axial flow compressors: a strategy for aerodynamic design and analysis. New York, USA: ASME Press, 2003.
33. Pachidis V. Gas turbine advanced performance simulation. PhD Thesis, Cranfield University, 2006.
34. Çetin M, Üçer AŞ, Hirsch C, Serovy GK. Application of modified loss and deviation correlations to transonic axial compressors. AGARD R745, 1987.
35. Creveling H. Axial-flow compressor computer program for calculating off-design performance. NASA CR-72472, 1968.
36. Urasek D, Gorrell W, Cunnan W. Performance of two-stage fan having low-aspect-ratio first stage rotor blading. NASA TP-1493, 1979.
37. Sullivan TJ, Younghans JL, Little DR. Single stage, low noise advanced technology fan. Volume 1: aerodynamic design. NASA CR-134801, 1976.
38. Sullivan T, Silverman I, Little D. Single stage, low noise advanced technology fan. Volume 4: fan aerodynamics. NASA CR-134892, 1977.
39. Casey M, Gersbach F, Robinson C. An optimization technique for radial compressor impellers. Proceedings of ASME Turbo Expo 2008, Berlin, Germany, 2008.
40. Zamboni G, Xu L. Fan root aerodynamics for large bypass gas turbine engines: influence on the engine performance and 3D design. Proceedings of ASME Turbo 2009, Florida, USA, 2009.